Appendix A.24:

St. Teresa's School – VsVp 57191

Table 1: Site Description for St. Teresa's School (VsVp 57191).

Attribute	Yes/No			Description/Date	Symbol in Figure 1
	10-m Buffer	20-m Buffer	50-m Buffer		
Near a body of surface water or other free face features?	No	No	No	The center of the site is ~500 m away from the Ilam Stream. The direction of the free face is roughly NW-SW, while its height is ~1 m.	NA
Lateral spreading observed during the CES?	No	No	No	NA	NA
Nearby buildings or structures?	No	Yes	Yes	Building coverage of the 10-m, 20-m, and 50-m buffers is 0, 10, and 24%, respectively. Buildings are in the N portion of the 20-m buffer and all quadrants of the 50-m buffer.	White Fill + Brown Outline
Sloping land?	No	No	No	Flat land, residential area.	NA
Step changes in the ground surface?	No	No	No	NA	NA
Retaining walls?	No	No	No	NA	NA
Vegetation?	Yes	Yes	Yes	Trees and bushes cover 18, 18, and 16% of the 10-, 20-, and 50-m buffers, respectively. They are in all quadrants of the buffers.	White Fill + Green Outline
Manmade changes to the site between the LiDAR surveys?	No	Yes	Yes	Building construction in the E portion of the 20- and 50-m buffers occurred between Apr 2012 and Oct 2012, affecting the Oct-2015 LiDAR survey.	Building Addition: Thin Yellow Outline
Other important factors?	Yes	Yes	Yes	Low-motor-vehicle-volume, two-way roadway (street) occupies 13% of the 50-m buffer and stretches throughout the NW and SW quadrants. The 50-m buffer captures 1% of the high-motor-vehicle-volume, two-way roadway in its SE and SW quadrants. Paved parking lot is in all quadrants of all three buffers. The overall coverage by the paved area (excludes buildings) is 83, 71, and 58 % for the 10-, 20-, and 50-m buffers, respectively.	Road 1: Gray Fill + Red Outline Road 2: White Fill + Gray Outline

Note: Buffer is the area within a circle of a specified radius with CPT investigations done at its center (172.592135°, -43.529873°).

Figure 1: Site plan with areas where ejecta-induced settlement is considered.

Note 1: Two patches and the road (outlined in red) in the free field were selected for settlement assessment as areas free of vegetation and structures. Other important factors considered in the patch selection process were its proximity to a CPT, to a property subjected to addition and/or demolition of a structure, front yard/backyard alterations (e.g., ploughing, rubble, scrap), and aerial distribution of sediment ejecta. However, the LiDAR-based settlement analyses were not conducted for any earthquake event due to the evident absence of ejecta from Patches A and B and Road.

Table 2: LiDAR flight error adjustments, global adjustments for the difference between average LiDAR point elevations and benchmark survey elevations, and vertical tectonic movement adjustments.

	Adjustments (mm)		
Earthquake Event(s)	LiDAR Flight Error	Global Offset[1]	Tectonic Vertical Movement
Sep-10	NA	-3	0
Feb-11	NA	16	-48
Jun-11	0	38	-20
Dec-11	0	-65	0
CES	-100	-14	-68
Any LiDAR survey affected by ejecta?			No

Note: The negative sign indicates the subtraction from the ground surface subsidence, while the positive sign indicates the addition to the ground surface subsidence.

Table 3a: LiDAR Measurement Error for Patch A.

Surveys	Buffer	Area Averaged Difference Indicating Repeat Measurement Error (mm)	$\sigma^*_{\text{individual LiDAR points}}$ (mm)	%Reduction in σ due to Area Averaging of LiDAR Points
Post Feb 2011: Mar 2011 and May 2011	10-m	ND	59	[ND,ND]
	20-m	ND		
	50-m	ND		
Post Dec 2011: Feb 2012 and Oct 2015	10-m	ND	70	[ND,ND]
	20-m	ND		
	50-m	ND		

*Standard deviation; ND = Not determined.

[1] Russell, J., & van Ballegooy, S. (2015). *Canterbury Earthquake Sequence: Increased liquefaction vulnerability assessment methodology*. New Zealand: Tonkin & Taylor Ltd.

Table 3b: LiDAR Measurement Error for Patch B and Road.

Surveys	Buffer	Area Averaged Difference Indicating Repeat Measurement Error (mm)	$\sigma^*_{\text{individual LiDAR points}}$ (mm)	%Reduction in σ due to Area Averaging of LiDAR Points
Post Feb 2011: Mar 2011 and May 2011	10-m	NA	59	[ND,ND]
	20-m	NA		
	50-m	ND		
Post Dec 2011: Feb 2012 and Oct 2015	10-m	NA	70	[ND,ND]
	20-m	NA		
	50-m	ND		

*Standard deviation; ND = Not determined.

Table 4a: Ground surface subsidence adjustments due to LiDAR measurement error for Patch A.

Earthquake Event(s)	$\sigma_{\text{pre-EQ LiDAR survey}}$ (mm)	$\sigma_{\text{post-EQ LiDAR survey}}$ (mm)	σ_{total} (mm)	Area Average Adjusted σ (mm) **
Sep-10	158	56	134	ND
Feb-11	56	59	59	ND
Jun-11	59	61	62	ND
Dec-11	61	70	87	ND
CES	158	70	124	ND

**Based on the highest %Reduction in Table 3a; ND = Not determined.

Table 4b: Ground surface subsidence adjustments due to LiDAR measurement error for Patch B and Road.

Earthquake Event(s)	$\sigma_{\text{pre-EQ LiDAR survey}}$ (mm)	$\sigma_{\text{post-EQ LiDAR survey}}$ (mm)	σ_{total} (mm)	Area Average Adjusted σ (mm) **
Sep-10	158	56	134	ND
Feb-11	56	59	59	ND
Jun-11	59	61	62	ND
Dec-11	61	70	87	ND
CES	158	70	124	ND

**Based on the highest %Reduction in Table 3b; ND = Not determined.

Table 5a: Raw liquefaction-related ground surface subsidence using original LiDAR points for Patch A.

Earthquake Event(s)	Average Ground Surface Subsidence (mm) 10-m Buffer	20-m Buffer	50-m Buffer
Sep-10	NA	NA	NA
Feb-11	NA	NA	NA
Jun-11	ND	ND	ND
Dec-11	ND	ND	ND
CES	ND	ND	ND

NA = Not available; ND = Not determined.

Table 5b: Raw liquefaction-related ground surface subsidence using original LiDAR points for Patch B and Road.

Earthquake Event(s)	Average Ground Surface Subsidence (mm) 10-m Buffer	20-m Buffer	50-m Buffer
Sep-10	NA	NA	NA
Feb-11	NA	NA	NA
Jun-11	NA	NA	ND
Dec-11	NA	NA	ND
CES	NA	NA	ND

Table 6a: Corrected liquefaction-related ground surface subsidence using original LiDAR points for Patch A with the calculated adjustments in Table 2.

Earthquake Event(s)	Average Calculated Ground Surface Subsidence (mm) 10-m Buffer	20-m Buffer	50-m Buffer
Sep-10	NA	NA	NA
Feb-11	NA	NA	NA
Jun-11	ND	ND	ND
Dec-11	ND	ND	ND
CES	ND	ND	ND

Notes: Plus/minus values are same as those in Table 4a, but rounded to the nearest 25; Positive overall values indicate ground surface subsidence, while negative overall values indicate ground surface uplift; NA = Not available; ND = Not determined.

Table 6b: Corrected liquefaction-related ground surface subsidence using original LiDAR points for Patch B and Road with the calculated adjustments in Table 2.

Earthquake Event(s)	Average Calculated Ground Surface Subsidence (mm)		
	10-m Buffer	20-m Buffer	50-m Buffer
Sep-10	NA	NA	NA
Feb-11	NA	NA	NA
Jun-11	NA	NA	ND
Dec-11	NA	NA	ND
CES	NA	NA	ND

Notes: Plus/minus values are same as those in Table 4b, but rounded to the nearest 25; Positive overall values indicate ground surface subsidence, while negative overall values indicate ground surface uplift; NA = Not available; ND = Not determined.

Table 7a: Corrected liquefaction-related ground surface subsidence for Patch A using LiDAR DEMs.

	Estimated Ground Surface Subsidence (mm)								
	10-m Buffer			20-m Buffer			50-m Buffer		
Earthquake Event(s)	16th %ile	50th %ile	84th %ile	16th %ile	50th %ile	84th %ile	16th %ile	50th %ile	84th %ile
Sep-10	NA	NA	NA	NA	NA	NA	NA	NA	NA
Feb-11	NA	NA	NA	NA	NA	NA	NA	NA	NA
Jun-11	<50	<50	<50	<50	<50	<50	<50	<50	<50
Dec-11	<50	<50	<50	<50	<50	<50	<50	<50	<50
CES	<50	<50	50	<50	50	50	<50	50	50

Note: These percentiles are not the exact statistical measures; they indicate the spatial variability of ground surface subsidence.

Table 7b: Corrected liquefaction-related ground surface subsidence for Patch B using LiDAR DEMs.

	Estimated Ground Surface Subsidence (mm)								
	10-m Buffer			20-m Buffer			50-m Buffer		
Earthquake Event(s)	16th %ile	50th %ile	84th %ile	16th %ile	50th %ile	84th %ile	16th %ile	50th %ile	84th %ile
Sep-10	NA	NA	NA	NA	NA	NA	NA	NA	NA
Feb-11	NA	NA	NA	NA	NA	NA	NA	NA	NA
Jun-11	NA	NA	NA	NA	NA	NA	<50	<50	<50
Dec-11	NA	NA	NA	NA	NA	NA	<50	<50	<50
CES	NA	NA	NA	NA	NA	NA	50	50	50

Note: These percentiles are not the exact statistical measures; they indicate the spatial variability of ground surface subsidence.

Table 7c: Corrected liquefaction-related ground surface subsidence for Road using LiDAR DEMs.

	Estimated Ground Surface Subsidence (mm)								
	10-m Buffer			20-m Buffer			50-m Buffer		
Earthquake Event(s)	16th %ile	50th %ile	84th %ile	16th %ile	50th %ile	84th %ile	16th %ile	50th %ile	84th %ile
Sep-10	NA	NA	NA	NA	NA	NA	NA	NA	NA
Feb-11	NA	NA	NA	NA	NA	NA	NA	NA	NA
Jun-11	NA	NA	NA	NA	NA	NA	<50	<50	<50
Dec-11	NA	NA	NA	NA	NA	NA	<50	<50	<50
CES	NA	NA	NA	NA	NA	NA	50	50	50

Note: These percentiles are not the exact statistical measures; they indicate the spatial variability of ground surface subsidence.

Table 8a: Ejecta-Induced settlement for the top 20 m of the soil profile for Patch A for the 50th %ile PGA, P_L=50%, and C_{FC}=0.13 using BI-2014, ZRB-2002, and I_C cutoff of 2.6.

Earthquake Event(s)	M_W	PGA (g)	Depth to Groundwater (m)	S_T (mm)	S_{V1D} (mm)	$S_{E,L}$ (mm)
Sep-10	7.1	0.22	0.8	NA	209±20	NA
Feb-11	6.2	0.34	0.9	NA	230±50	NA
Jun-11	6.2	0.17	0.9	ND	80±25	ND
Dec-11	6.1	0.16	0.8	ND	61±50	ND

Notes: S_T = Total settlement (Table 6); S_{V1D} = Average vertical settlement due to volumetric compression using Boulanger and Idriss (2014) (BI-2014), Zhang et al. (2002) (ZRB-2002) procedures and de Greef and Lengkeek (2018) thin-layer correction; $S_{E,L}$ = Ejecta-induced settlement as the difference between the LiDAR-based S_T and S_{V1D}.

Table 8b: Ejecta-Induced settlement for the top 20 m of the soil profile for Patch B for the 50th %ile PGA, P_L=50%, and C_{FC}=0.13 using BI-2014, ZRB-2002, and I_C cutoff of 2.6.

Earthquake Event(s)	M_W	PGA (g)	Depth to Groundwater (m)	S_T (mm)	S_{V1D} (mm)	$S_{E,L}$ (mm)
Sep-10	7.1	0.22	0.8	NA	209±20	NA
Feb-11	6.2	0.34	0.9	NA	230±50	NA
Jun-11	6.2	0.17	0.9	ND	80±25	ND
Dec-11	6.1	0.16	0.8	ND	61±50	ND

Notes: S_T = Total settlement (Table 6); S_{V1D} = Average vertical settlement due to volumetric compression using Boulanger and Idriss (2014) (BI-2014), Zhang et al. (2002) (ZRB-2002) procedures and de Greef and Lengkeek (2018) thin-layer correction; $S_{E,L}$ = Ejecta-induced settlement as the difference between the LiDAR-based S_T and S_{V1D}.

Table 8c: Ejecta-Induced settlement for the top 20 m of the soil profile for Road for the 50th %ile PGA, P_L=50%, and C_{FC}=0.13 using BI-2014, ZRB-2002, and I_C cutoff of 2.6.

Earthquake Event(s)	M_W	PGA (g)	Depth to Groundwater (m)	S_T (mm)	S_{V1D} (mm)	$S_{E,L}$ (mm)
Sep-10	7.1	0.22	0.8	NA	208±20	NA
Feb-11	6.2	0.34	0.9	NA	231±50	NA
Jun-11	6.2	0.17	0.9	ND	75±25	ND
Dec-11	6.1	0.16	0.8	ND	56±50	ND

Notes: S_T = Total settlement (Table 6); S_{V1D} = Average vertical settlement due to volumetric compression using Boulanger and Idriss (2014) (BI-2014), Zhang et al. (2002) (ZRB-2002) procedures and de Greef and Lengkeek (2018) thin-layer correction; $S_{E,L}$ = Ejecta-induced settlement as the difference between the LiDAR-based S_T and S_{V1D}.

Note 2: The uncertainty for volumetric settlement was derived based on the sensitivity of volumetric settlement to PGA, C_{FC}, and P_L for each earthquake event for VsVp 57203 *Shirley Intermediate School* and CC LIQ 1 – CPT 5586 – *Vivian St* sites. Taking the 50th percentile as the baseline case, the minimum and maximum values corresponding to the difference between the 25th percentile and the 50th percentile and the 75th percentile and the 50th percentile were determined. The arithmetic mean of the range of the minimum and maximum difference was evaluated for each patch at the two sites. The maximum arithmetic mean for each earthquake event was rounded to the nearest five and used as the uncertainty value. Accordingly, the 1-D volumetric settlement uncertainties of ±20, ±50, ±25, and ±50 mm for the Sep-10, Feb-11, Jun-11, and Dec-11 earthquake events, respectively, were used for all sites in this study.

Table 9a: Coverage area and height of ejecta estimates for Patch A (10-m/20-m/50-m buffers) using photographs.

Earthquake Event	$A_{E,thick}$ (m^2)	$H_{E,thick}$ (mm)	$A_{E,thin}$ (m^2)	$H_{E,thin}$ (mm)	A_T (m^2)
Sep-10	0	0	0	0	147/326/367
Feb-11	0	0	0	0	147/326/367
Jun-11	0	0	0	0	147/326/367
Dec-11*	0	0	0	0	147/326/367

Notes: $A_{E,thick/thin}$ = Coverage area of thick/thin ejecta layers; $H_{E,thick/thin}$ = Lower-upper estimate of height of thick/thin ejecta layers; A_T = Total assessment area of a buffer being considered; Thin and thick layers correspond to light gray and dark gray colors of ejecta observed in aerial photographs; * indicates uncertainty due to the lack of physical evidence.

Table 9b: Coverage area and height of ejecta estimates for Patch B (50-m buffer) using photographs.

Earthquake Event	$A_{E,thick}$ (m^2)	$H_{E,thick}$ (mm)	$A_{E,thin}$ (m^2)	$H_{E,thin}$ (mm)	A_T (m^2)
Sep-10	0	0	0	0	157
Feb-11	0	0	0	0	157
Jun-11	0	0	0	0	157
Dec-11*	0	0	0	0	157

Notes: $A_{E,thick/thin}$ = Coverage area of thick/thin ejecta layers; $H_{E,thick/thin}$ = Lower-upper estimate of height of thick/thin ejecta layers; A_T = Total assessment area of a buffer being considered; Thin and thick layers correspond to light gray and dark gray colors of ejecta observed in aerial photographs; * indicates uncertainty due to the lack of physical evidence.

Table 9c: Coverage area and height of ejecta estimates for Road (50-m buffer) using photographs.

Earthquake Event	$A_{E,thick}$ (m^2)	$H_{E,thick}$ (mm)	$A_{E,thin}$ (m^2)	$H_{E,thin}$ (mm)	A_T (m^2)
Sep-10	0	0	0	0	998
Feb-11	0	0	0	0	998
Jun-11	0	0	0	0	998
Dec-11*	0	0	0	0	998

Notes: $A_{E,thick/thin}$ = Coverage area of thick/thin ejecta layers; $H_{E,thick/thin}$ = Lower-upper estimate of height of thick/thin ejecta layers; A_T = Total assessment area of a buffer being considered; Thin and thick layers correspond to light gray and dark gray colors of ejecta observed in aerial photographs; * indicates uncertainty due to the lack of physical evidence.

Note 3: The values in Table 9 are based on satellite and aerial photographs (Figures 8, 9, and 19 through 21) showing no ejecta at the site. There are no EQC LDAT property inspection reports. The ejecta-induced settlement using photographs and engineering judgment, $S_{E,P}$, is estimated as

$$S_{E,P} = \frac{\sum_{i=1}^{a} A_{E,thick,i} * H_{E,thick,i} + \sum_{j=1}^{b} A_{E,thin,j} * H_{E,thin,j}}{A_T} = \frac{\sum_{i=1}^{a} V_{E,thick,i} + \sum_{j=1}^{b} V_{E,thin,j}}{A_T}$$

where

- $A_{E,thick,i}$ and $H_{E,thick,i}$ are the area and the height of a thick ejecta layer, respectively;
- $A_{E,thin,j}$ and $H_{E,thin,j}$ are the area and the height of a thin ejecta layer, respectively;
- A_T is the total assessment area for a buffer being considered (Figure 1).

Table 10: Ejecta-induced settlement estimates for Patches A and B and Road based on photographs.

Earthquake Event	Patch A (10-, 20-, and 50-m buffers)		Patch B (50-m buffer)		Road (50-m buffer)	
	$S_{E,P,lower}$ (mm)	$S_{E,P,upper}$ (mm)	$S_{E,P,lower}$ (mm)	$S_{E,P,upper}$ (mm)	$S_{E,P,lower}$ (mm)	$S_{E,P,upper}$ (mm)
Sep-10	0	0	0	0	0	0
Feb-11	0	0	0	0	0	0
Jun-11	0	0	0	0	0	0
Dec-11*	0	0	0	0	0	0

Notes: $S_{E,P,lower}$ and $S_{E,P,upper}$ correspond to lower and upper estimates of $S_{E,P}$, respectively; * indicates uncertainty due to the lack of physical evidence.

Table 11: Best final estimates of ejecta-induced settlement for Patches A and B and Road.

EQ Event	Patch A (10-, 20-, and 50-m buffers)			Patch B (50-m buffer)			Road (50-m buffer)		
	$S_{E,L}$ (mm)	$S_{E,P}$ (mm)	$S_{E,final}$ (mm)	$S_{E,L}$ (mm)	$S_{E,P}$ (mm)	$S_{E,final}$ (mm)	$S_{E,L}$ (mm)	$S_{E,P}$ (mm)	$S_{E,final}$ (mm)
Sep-10	NA	0	0	NA	0	0	NA	0	0
Feb-11	NA	0	0	NA	0	0	NA	0	0
Jun-11	ND	0	0	ND	0	0	ND	0	0
Dec-11	ND	0	0*	ND	0	0*	ND	0	0*

Notes: $S_{E,L}$ = Ejecta-induced settlement based on LiDAR data reported in Table 8; $S_{E,P}$ = Median ejecta-induced settlement for the range of values reported in Table 10; $S_{E,final}$ = Best final estimate of ejecta-induced settlement rounded to the nearest 5; Final plus/minus values are also rounded to the nearest 5; * indicates uncertainty due to the lack of physical evidence.

Note 4:

- $S_{E,final}$ for Patches A and B and Road is based solely on $S_{E,P}$ for all earthquake events due to the evident absence of ejecta.
- The Maurer et al. (2014)[2] LPI prediction error is not available for the site.

<u>**Summary**</u>:

The best estimate of the ejecta-induced free-field ground settlement at the St. Teresa's School site for the SEP 2010, FEB 2011, JUN 2011, and DEC 2011 earthquake is 0 mm, 0 mm, 0 mm, and 0 mm, respectively.

[2] Maurer, B. W., Green, R. A., Cubrinovski, M., & Bradley, B. A. (2014). Evaluation of the Liquefaction Potential Index for Assessing Liquefaction Hazard in Christchurch, New Zealand. *Journal of Geotechnical and Geoenvironmental Engineering*, 140(7), 04014032-1-11. doi:10.1061/(asce)gt.1943-5606.0001117

Figure 2: Location of the site.

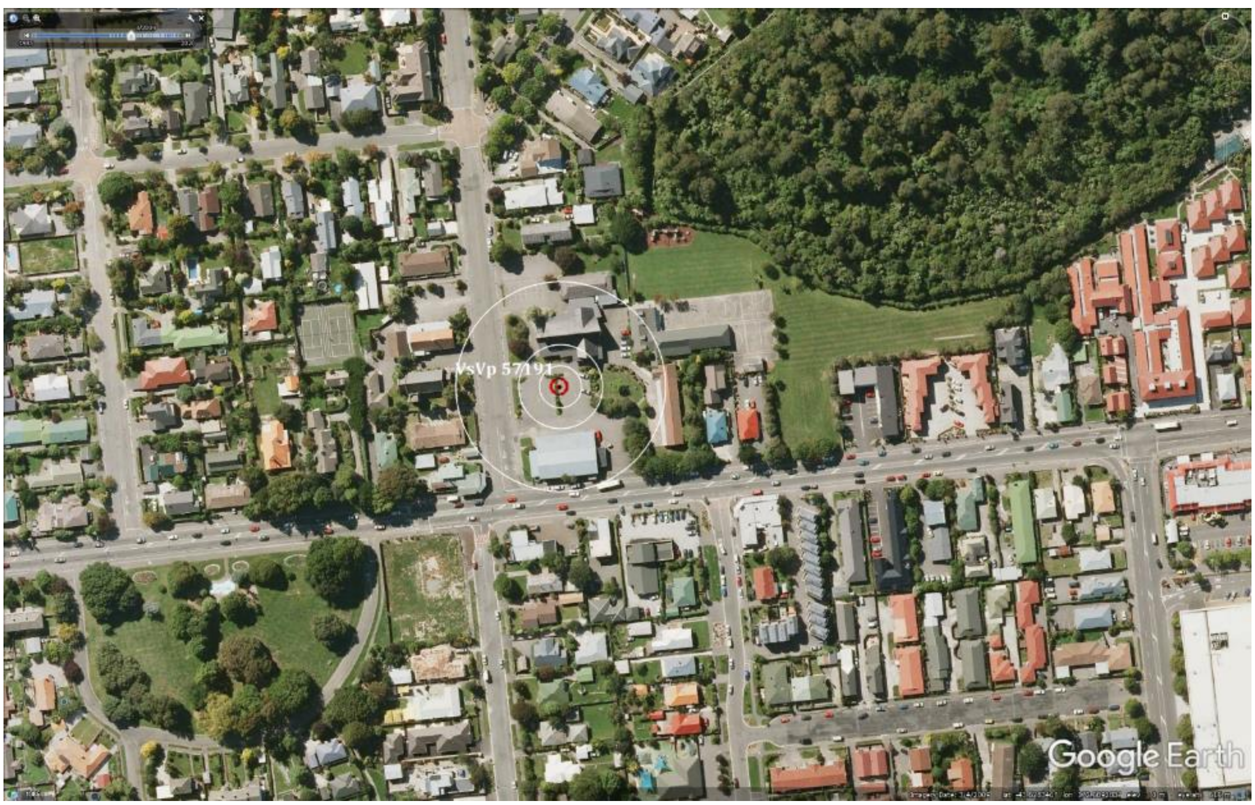

Figure 3: Position of the site relative to nearby buildings and vegetation.

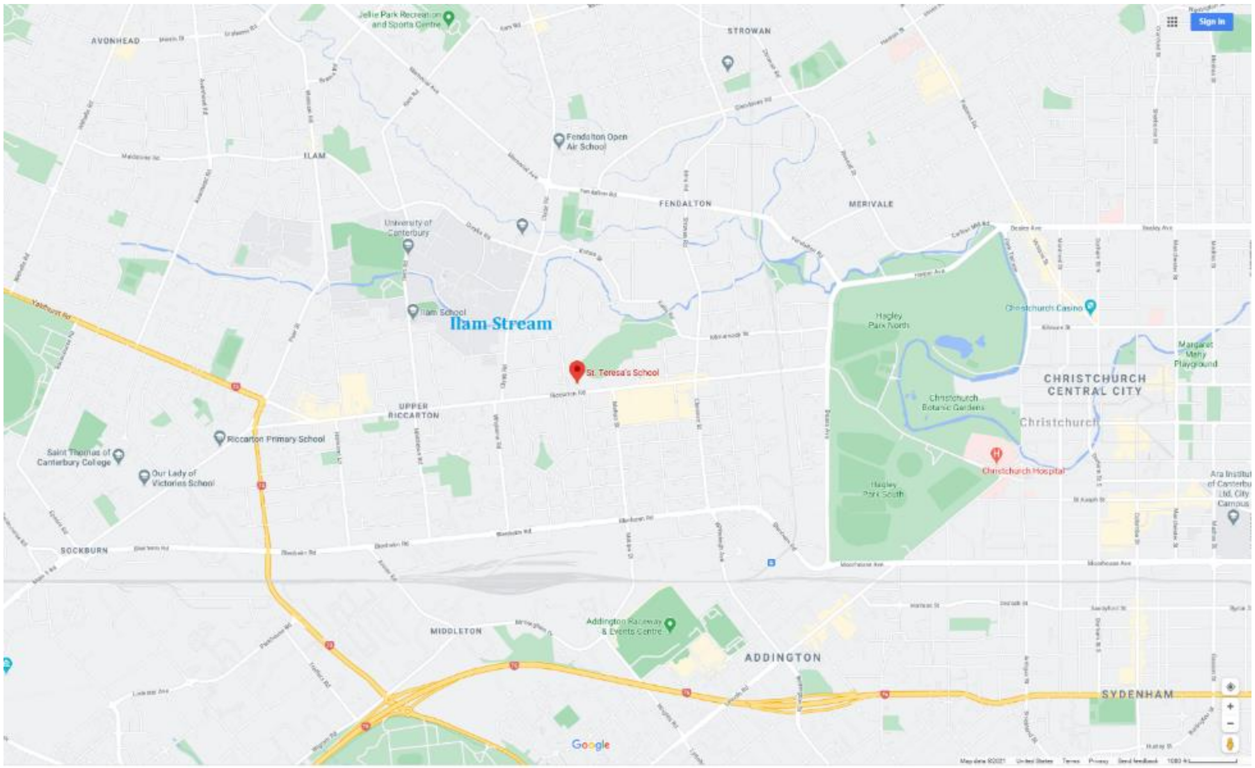

Figure 4: Position of the site relative to nearby buildings, vegetation, and free-face features.

Figure 5: Street view of the flat land.

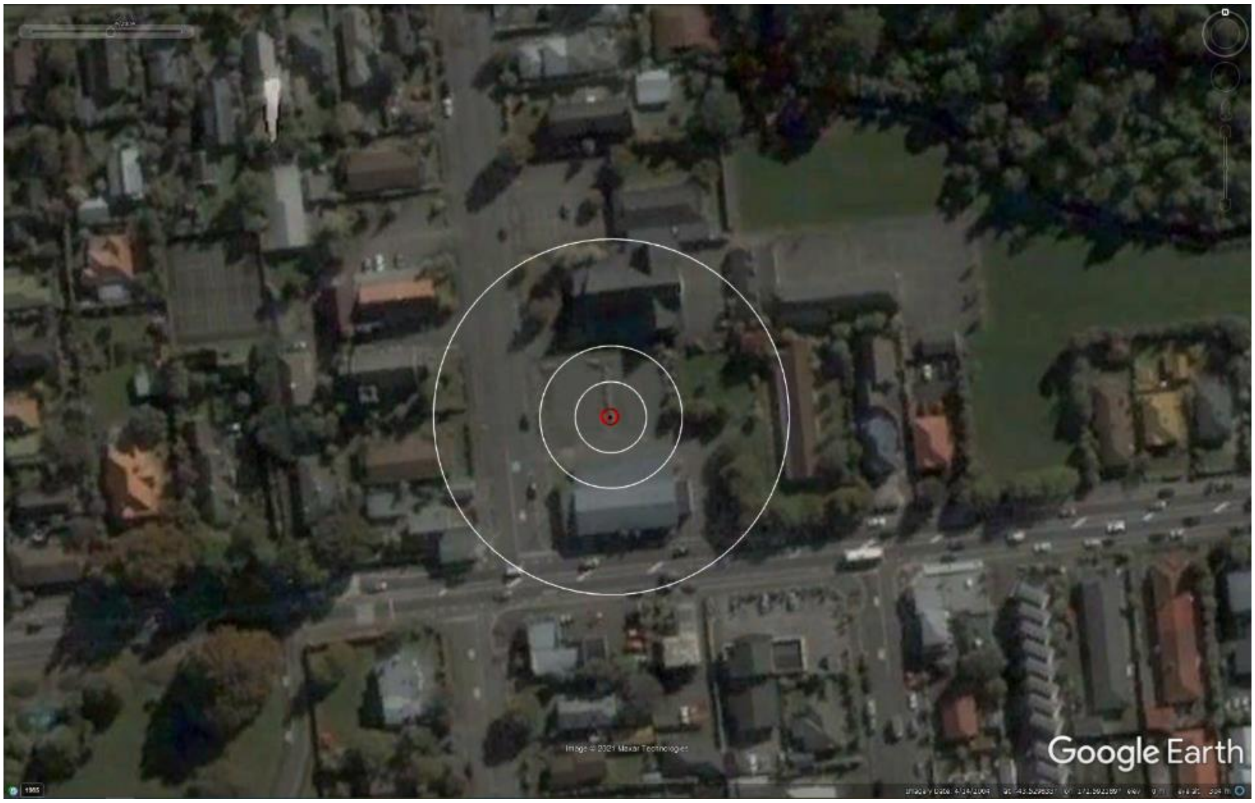

Figure 6: Satellite image of the site taken in Apr 2004.

Figure 7: Satellite image of the site taken in Mar 2009.

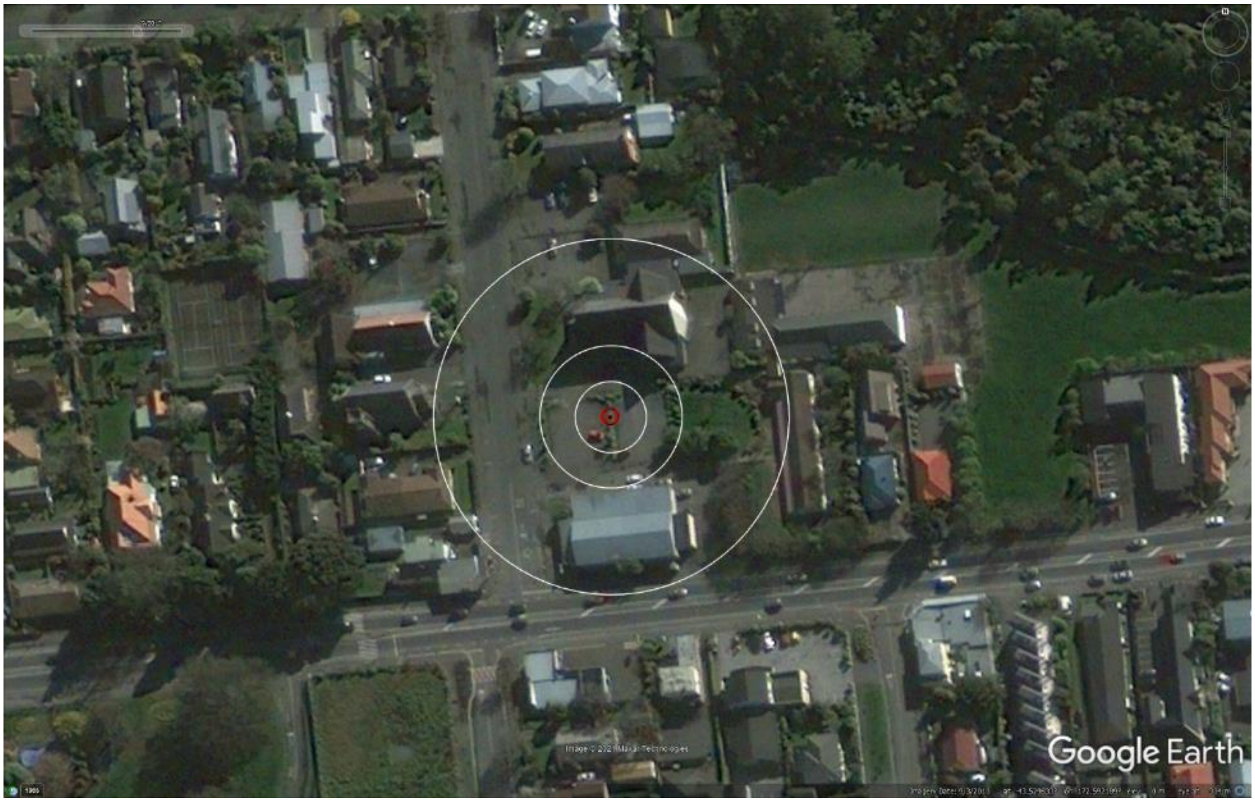

Figure 8: Satellite image of the site taken on Sep 3, 2010.

Figure 9: Satellite image of the site taken on Sep 5, 2010.

Figure 10: Satellite image of the site taken on Feb 7, 2011.

Figure 11: Satellite image of the site taken on Feb 23, 2011.

Figure 12: Satellite image of the site taken on Feb 26, 2011.

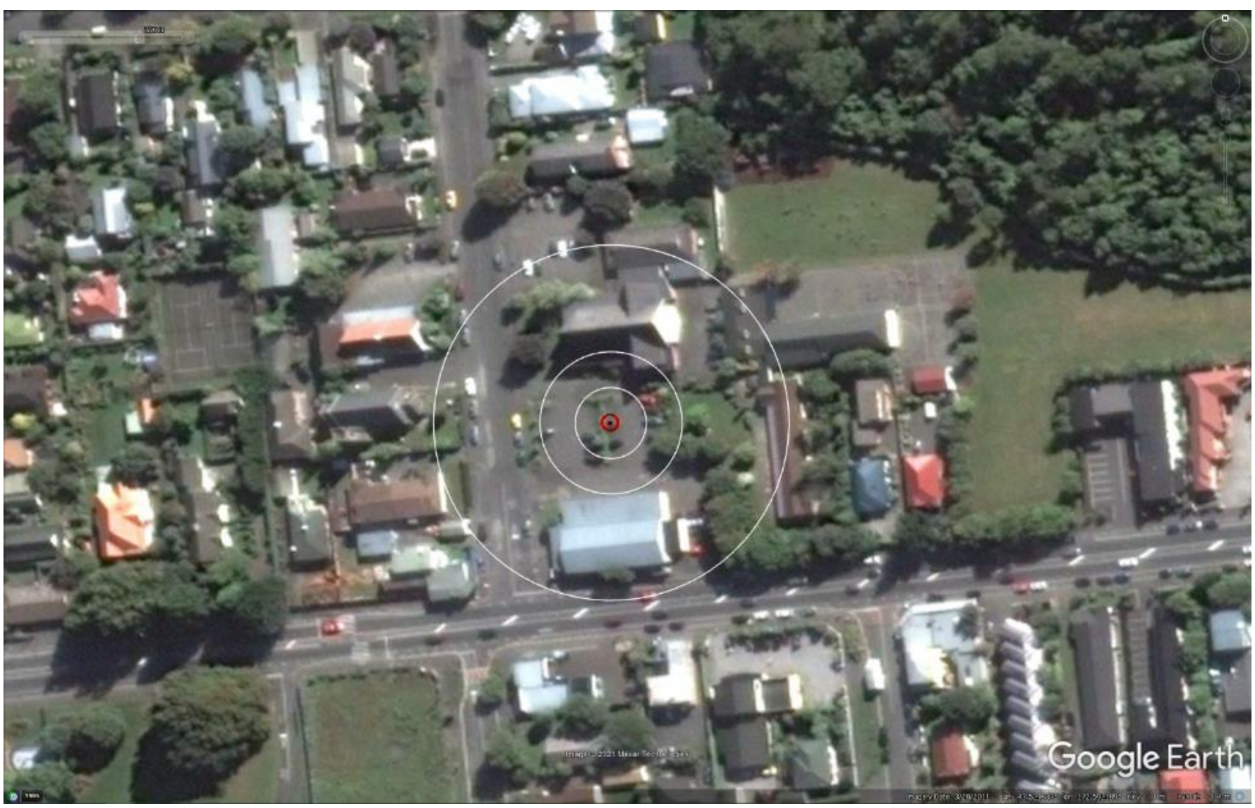

Figure 13: Satellite image of the site taken in Mar 2011.

Figure 14: Satellite image of the site taken in Aug 2011.

Figure 15: Satellite image of the site taken in Apr 2012.

Figure 16: Satellite image of the site taken in Oct 2012.

Figure 17: Satellite image of the site taken in Jan 2016.

Figure 18: Aerial photograph of the site taken on Sep 4, 2010.

Figure 19: Aerial photograph of the site taken on Feb 24, 2011.

Figure 20: Aerial photograph of the site taken on June 14-15, 2011.

Figure 21: Aerial photograph of the site taken on June 16, 2011.

Figure 22: Aerial photograph of the site taken on Dec 24, 2011.

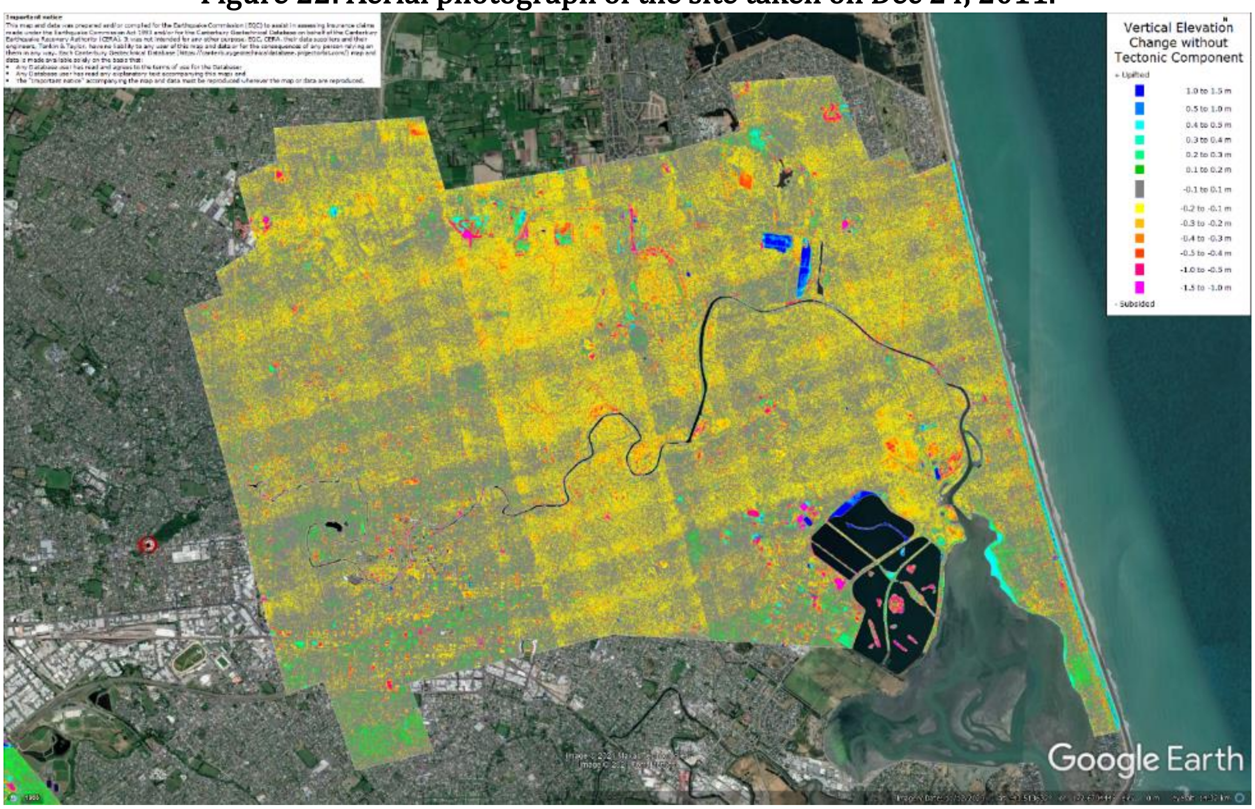

Figure 23: Vertical Ground Movements (Surface – Tectonic) for Sep 2010 Earthquake were not captured by the Sep 2010 LiDAR survey.

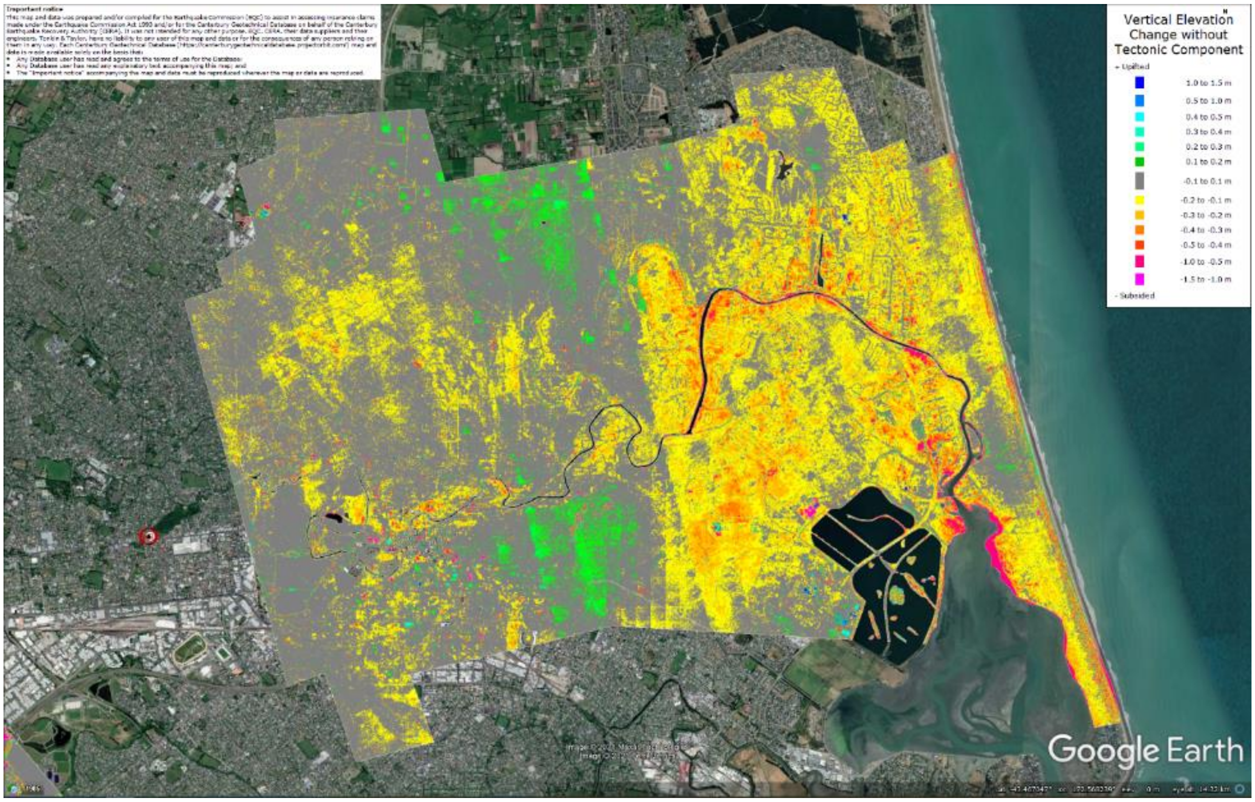

Figure 24: Vertical Ground Movements (Surface – Tectonic) for Feb 2011 Earthquake were not captured by the Sep 2010 LiDAR survey.

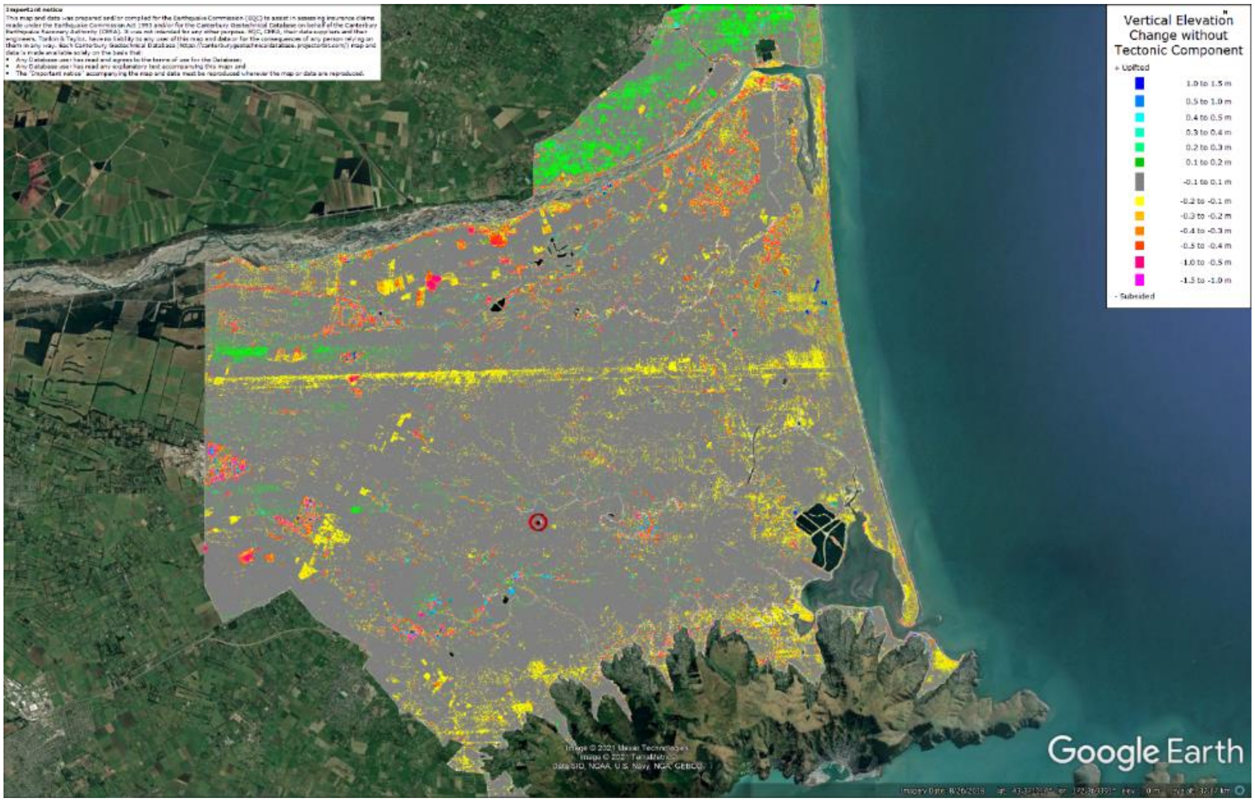

Figure 25: Vertical Ground Movements (Surface – Tectonic) for June 2011 Earthquake – the site is not in the apparent zone of overestimated or underestimated ground surface subsidence.

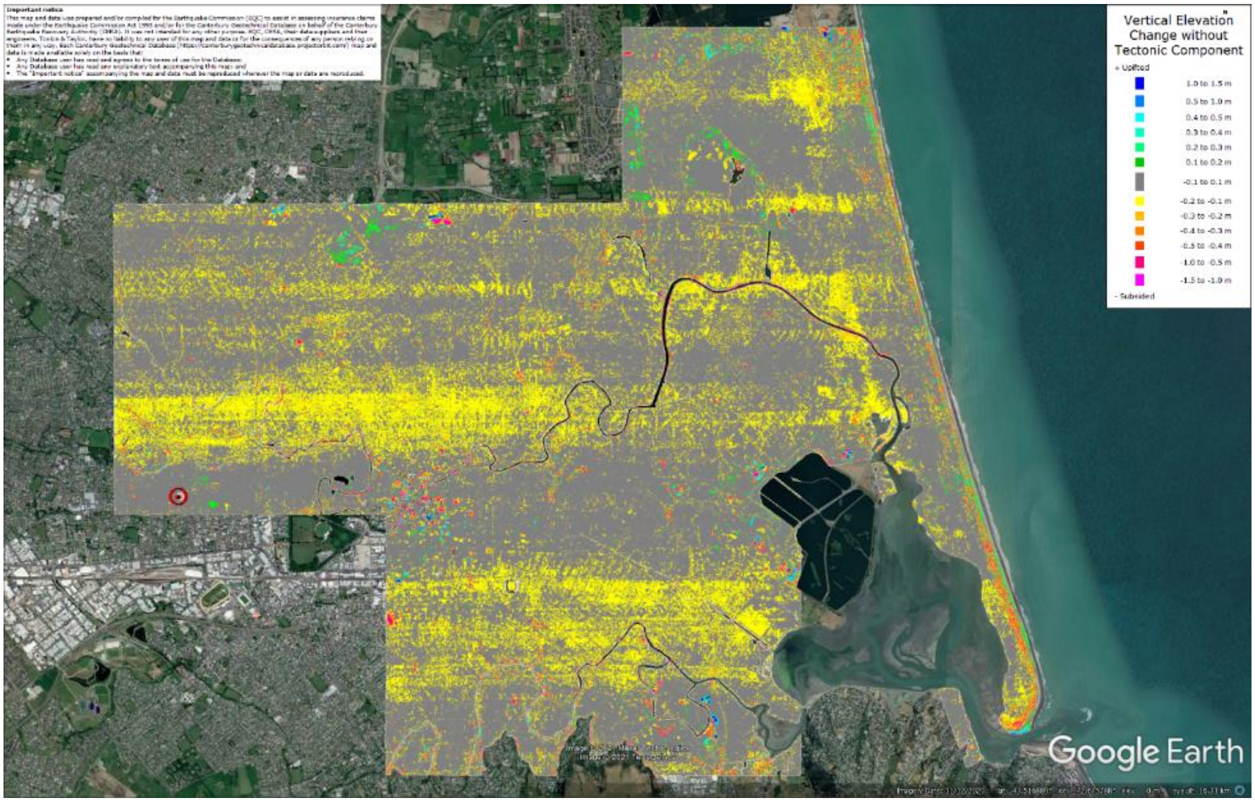

Figure 26: Vertical Ground Movements (Surface – Tectonic) for Dec 2011 Earthquake – the site is not in the apparent zone of overestimated or underestimated ground surface subsidence.

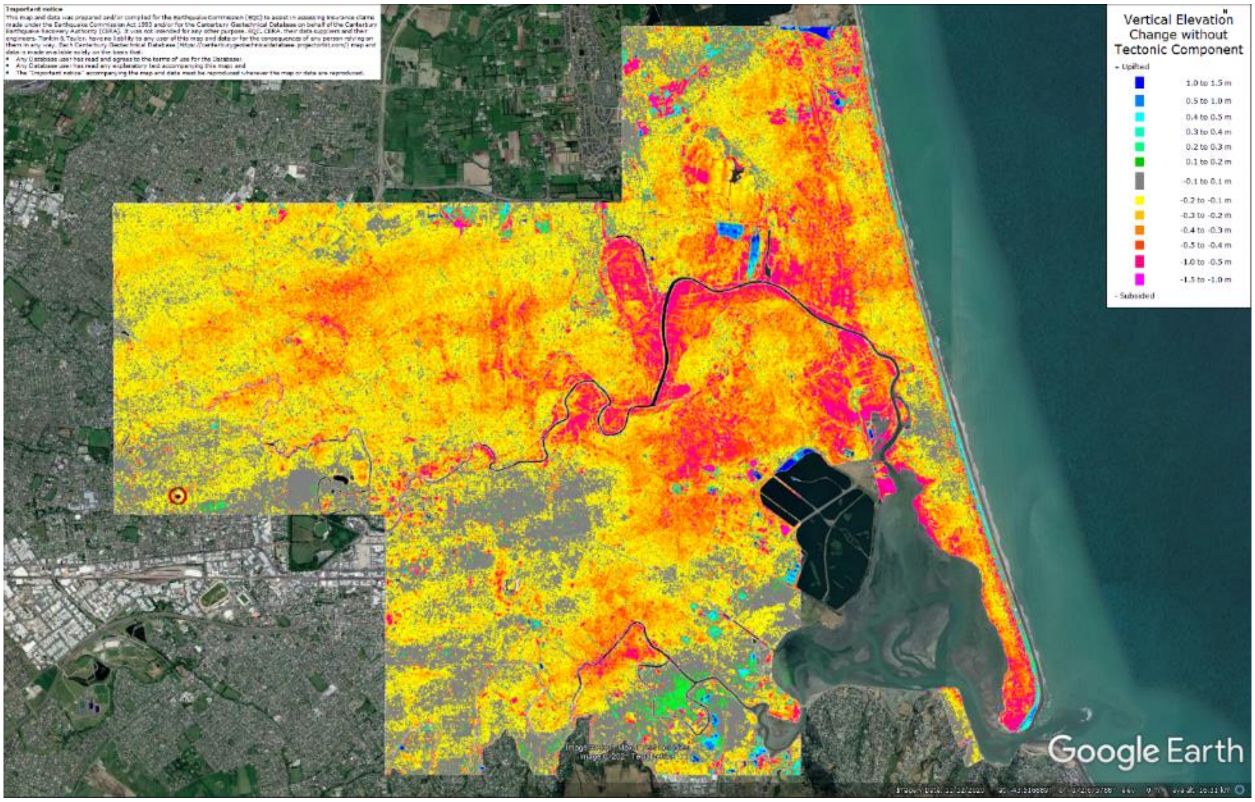

Figure 27: Vertical Ground Movements (Surface – Tectonic) for CES – the site is in the apparent zone of overestimated ground surface subsidence (i.e., July 2003 LiDAR flight error).

Note 5: The LiDAR DEM ground surface subsidence without tectonic component is not available for the Sep 2010 and Feb 2011 Earthquakes.

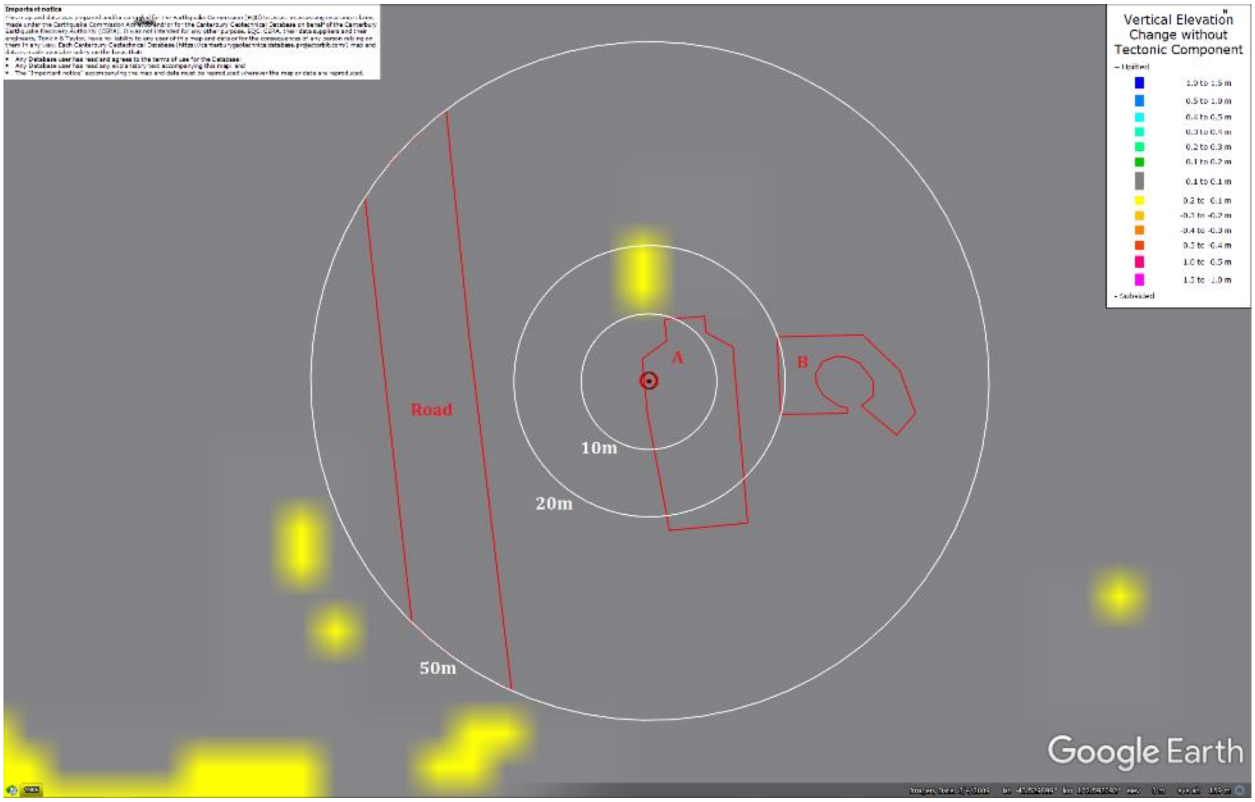

Figure 28: Ground surface subsidence without tectonic component for June 2011 Earthquake according to the LiDAR DEM.

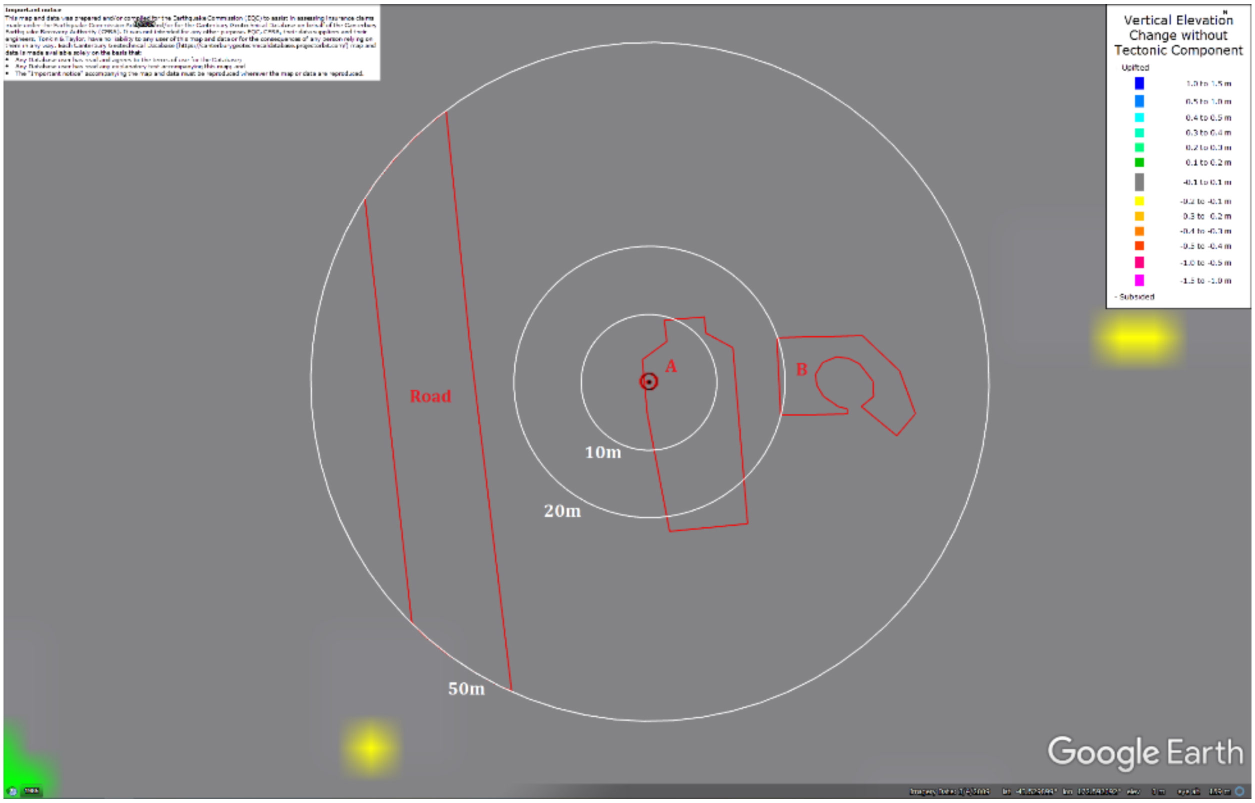

Figure 29: Ground surface subsidence without tectonic component for Dec 2011 Earthquake according to the LiDAR DEM.

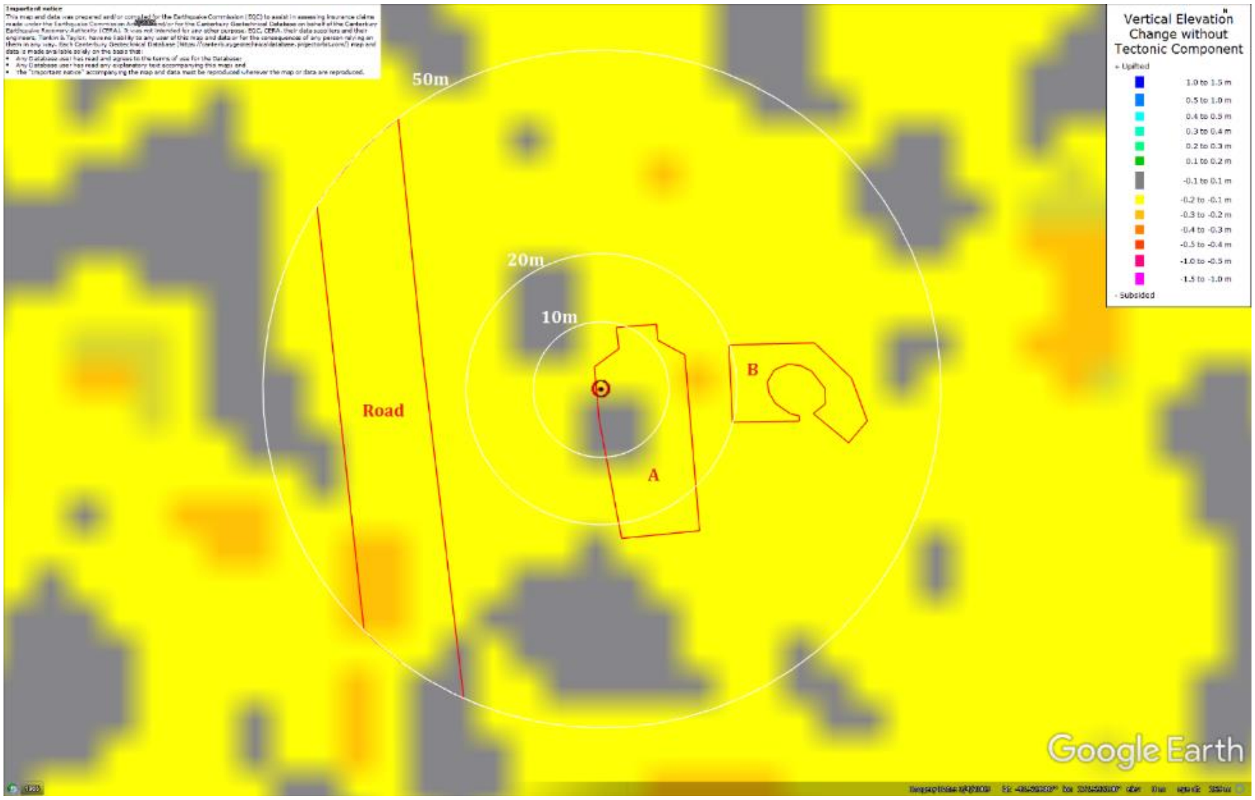

Figure 30: Ground surface subsidence without tectonic component for Canterbury Earthquake Sequence according to the LiDAR DEM.

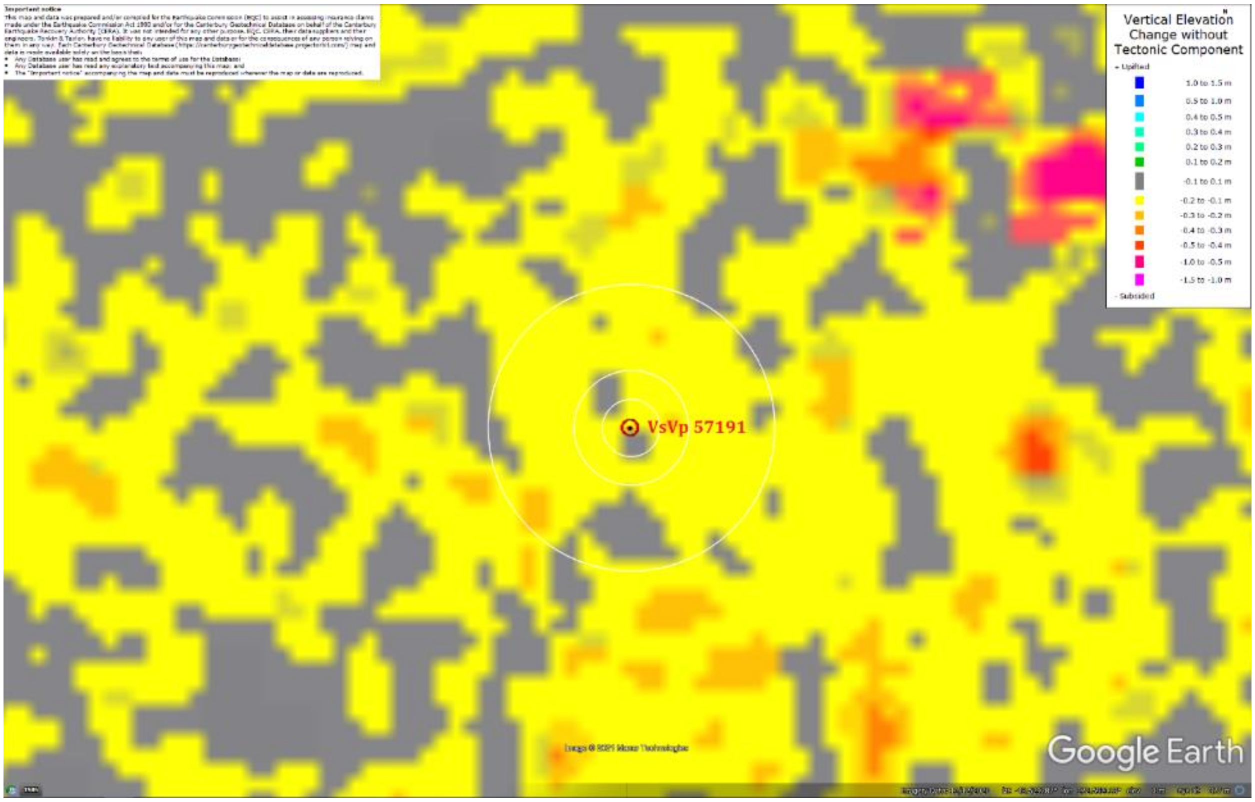

Figure 31: No lateral spreading for Canterbury Earthquake Sequence.

Figure 32: Vertical tectonic movements for Sep 2010 Earthquake.

Figure 33: Vertical tectonic movements for Feb 2011 Earthquake.

Figure 34: Vertical tectonic movements for June 2011 Earthquake.

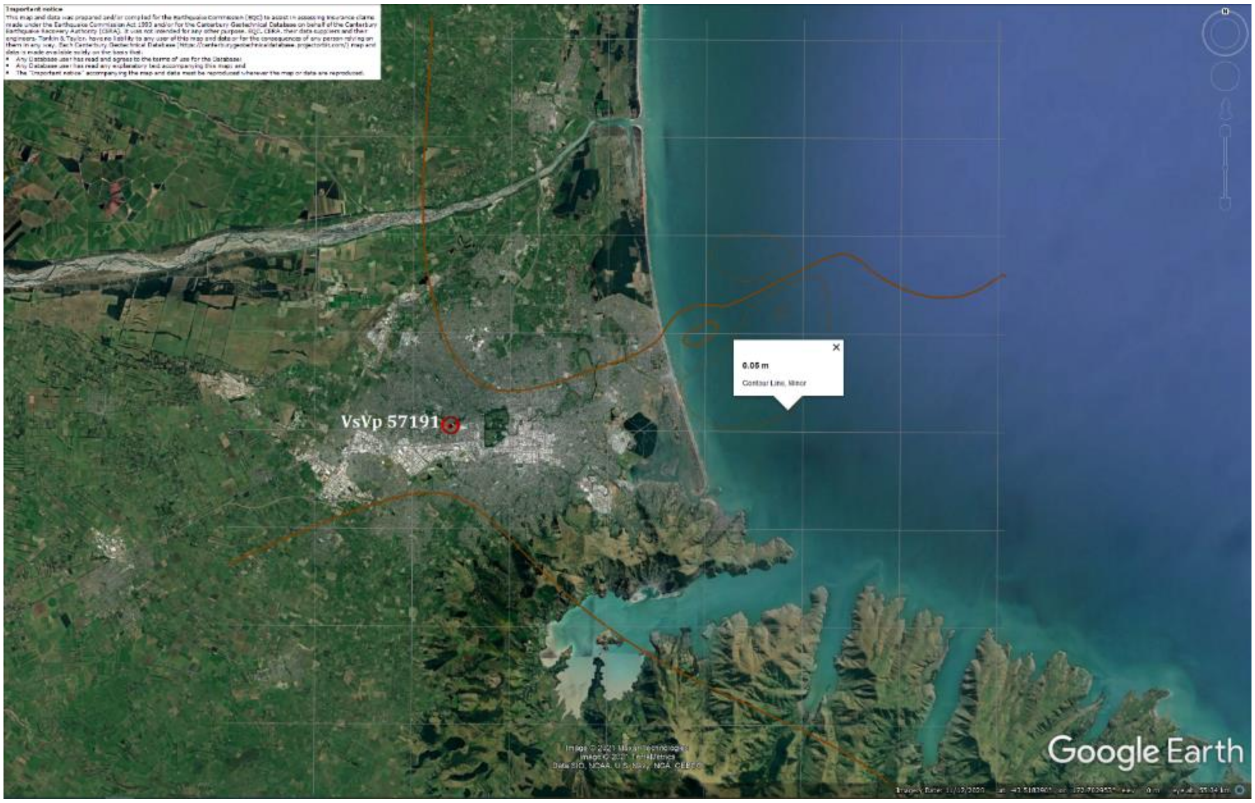

Figure 35: Vertical tectonic movements for Dec 2011 Earthquake.

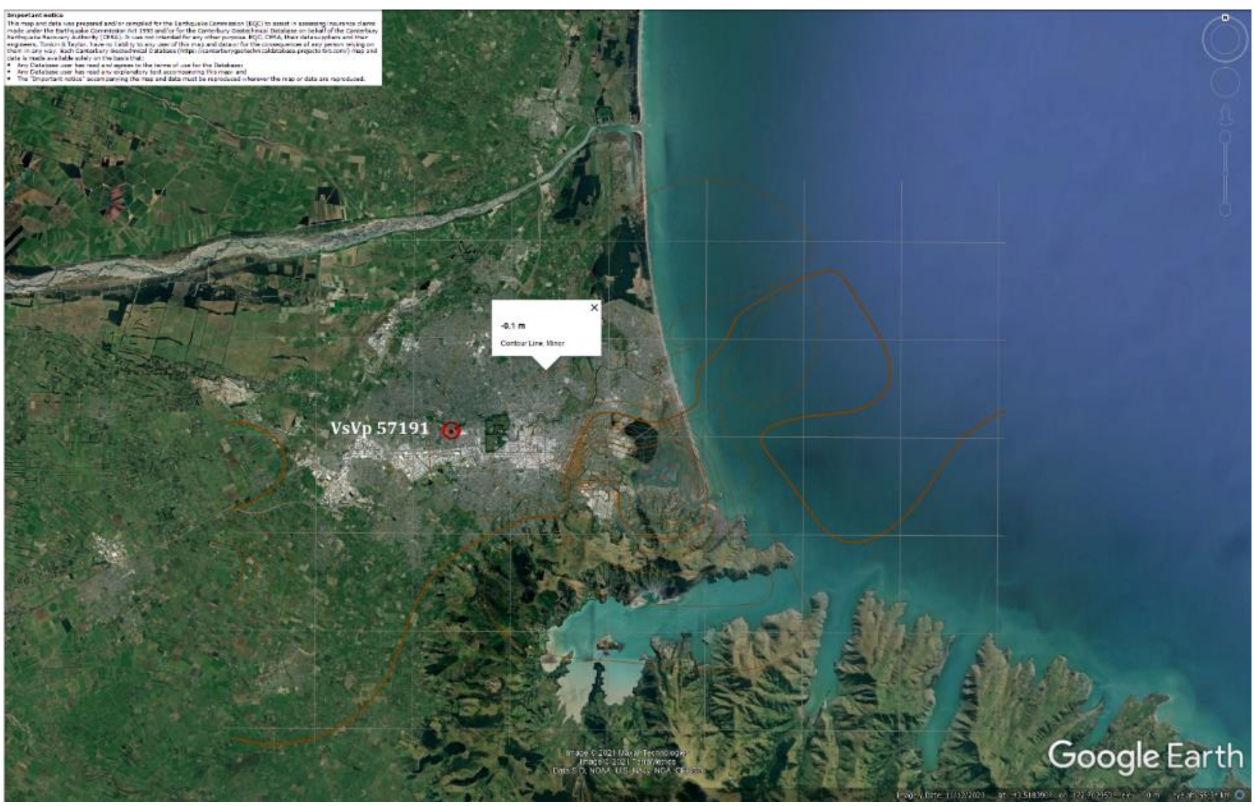

Figure 36: Vertical tectonic movements for Canterbury Earthquake Sequence.

Figure 37: PGA for Sep-10 EQ (st. dev. = 0.325-0.350 ln units).

Figure 38: PGA for Feb-11 EQ (st. dev. = 0.350-0.375 ln units).

Figure 39: PGA for Jun-11 EQ (st. dev. = 0.375-0.400 ln units).

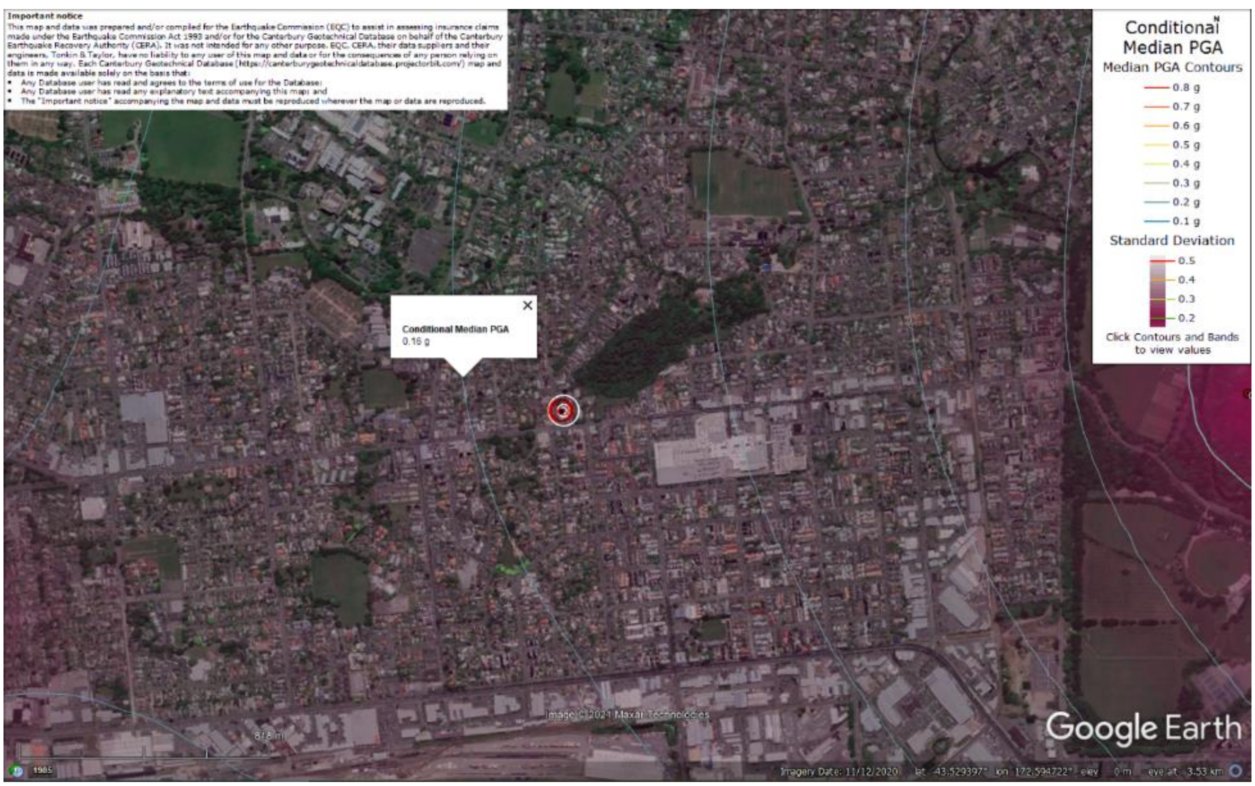

Figure 40: PGA for Dec-11 EQ (st. dev. = 0.375-0.400 ln units).

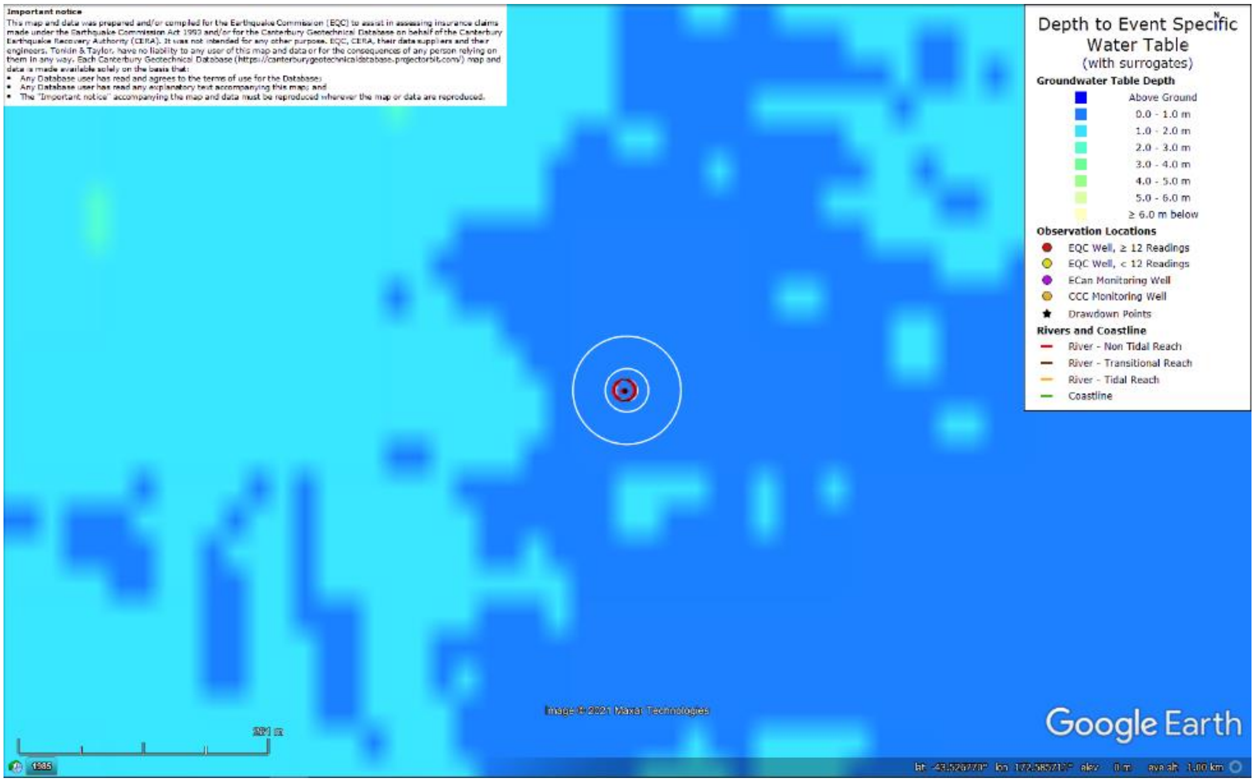

Figure 41: Depth to groundwater table for Sep-10 EQ.

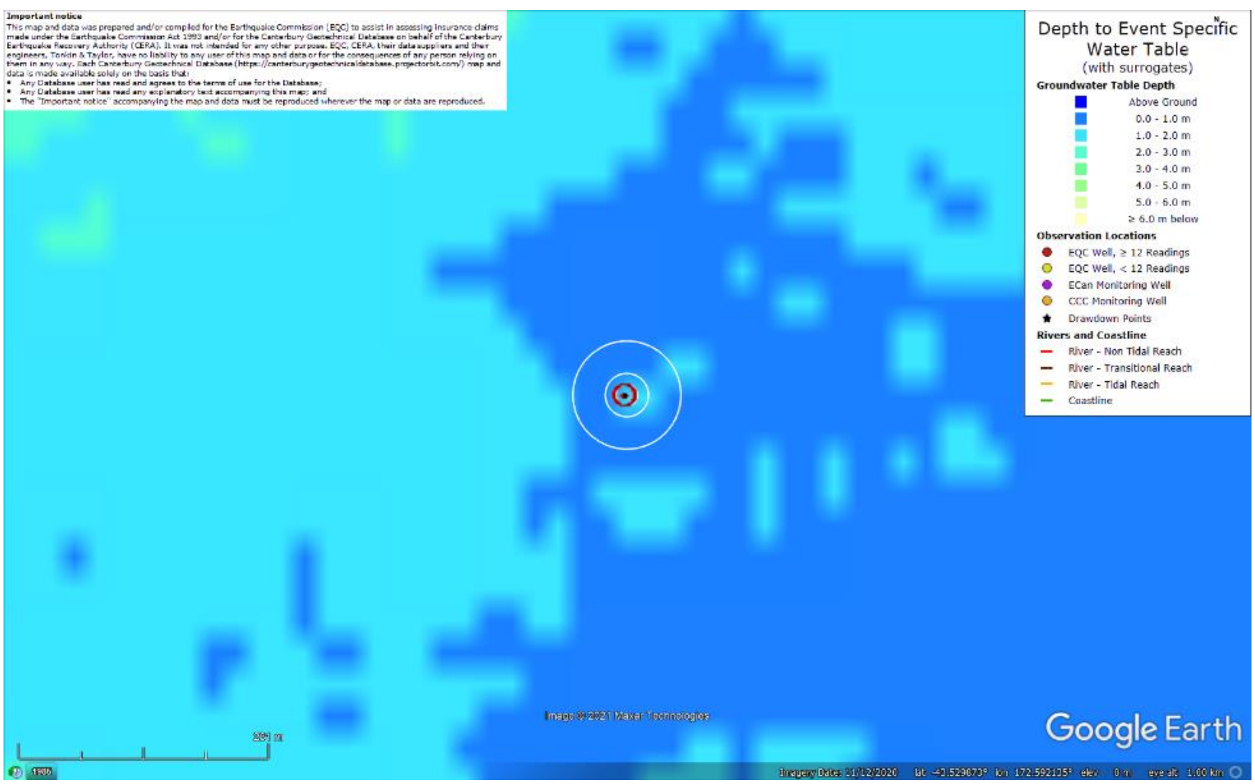

Figure 42: Depth to groundwater table for Feb-11 EQ.

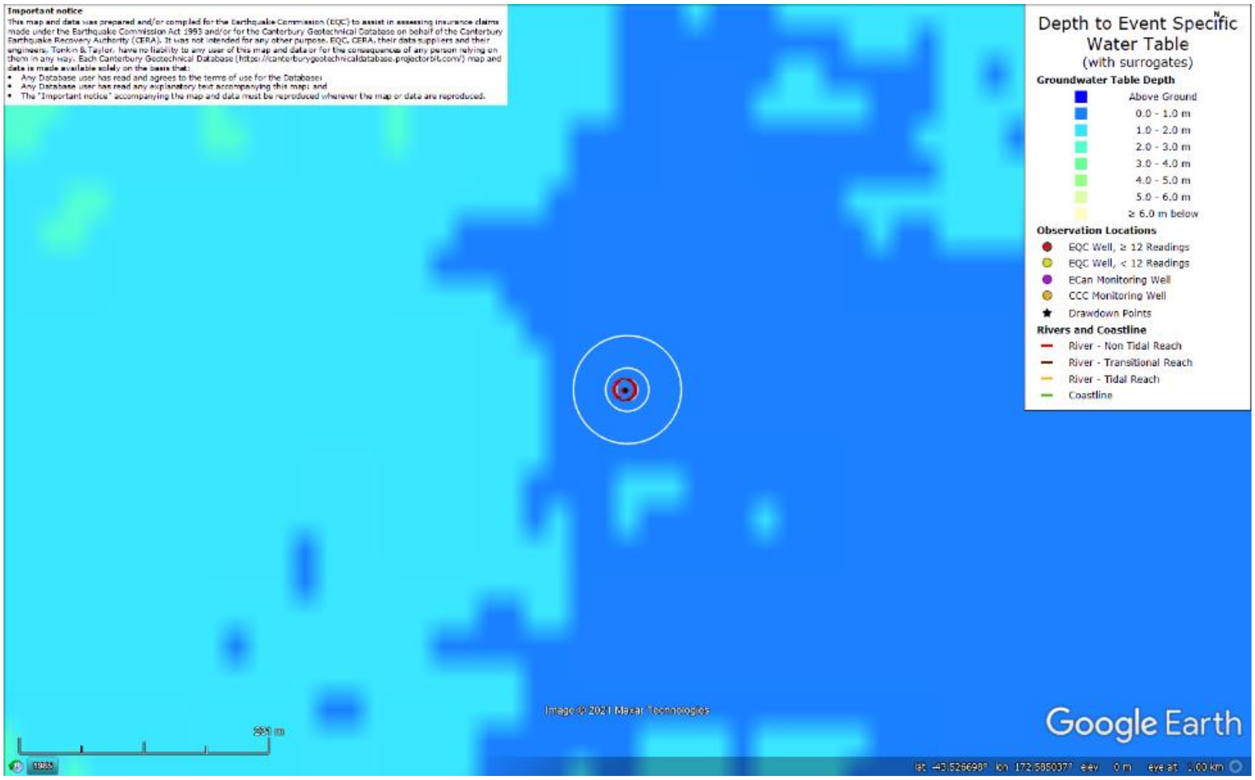

Figure 43: Depth to groundwater table for Jun-11 EQ.

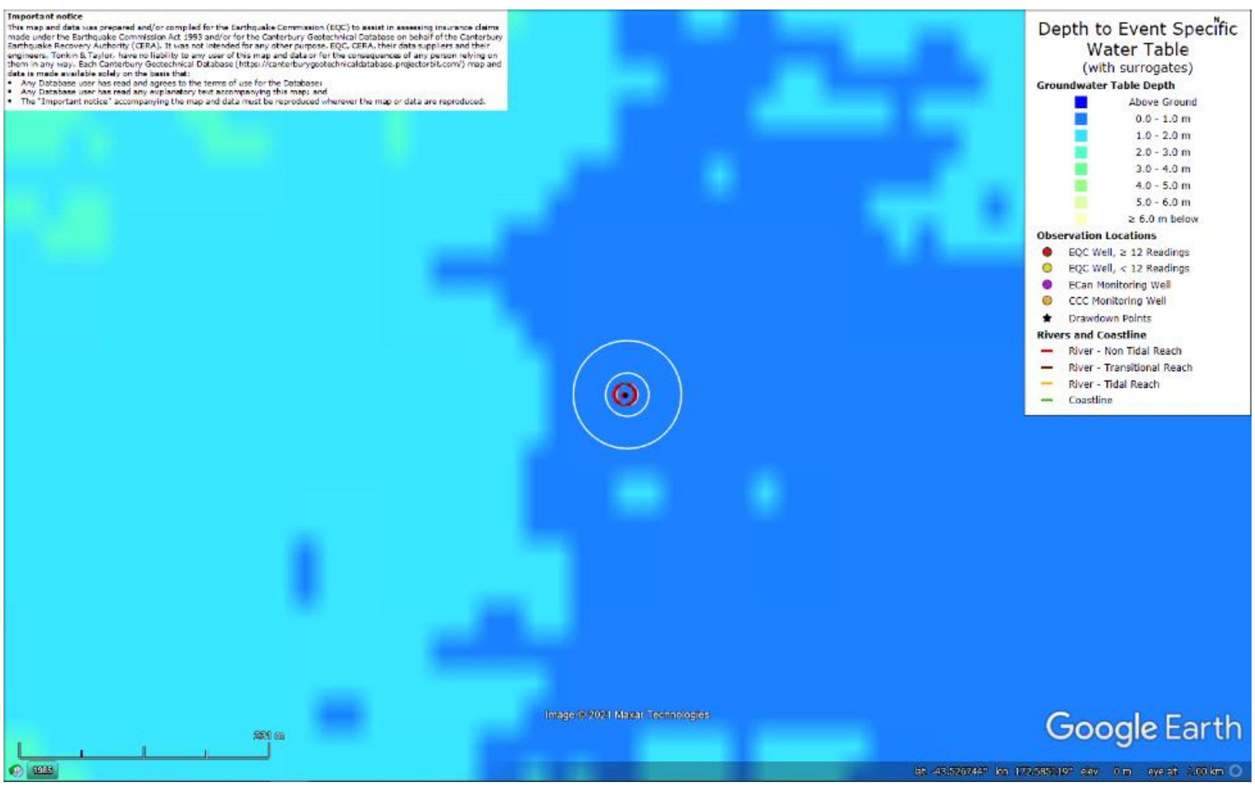

Figure 44: Depth to groundwater table for Dec-11 EQ.

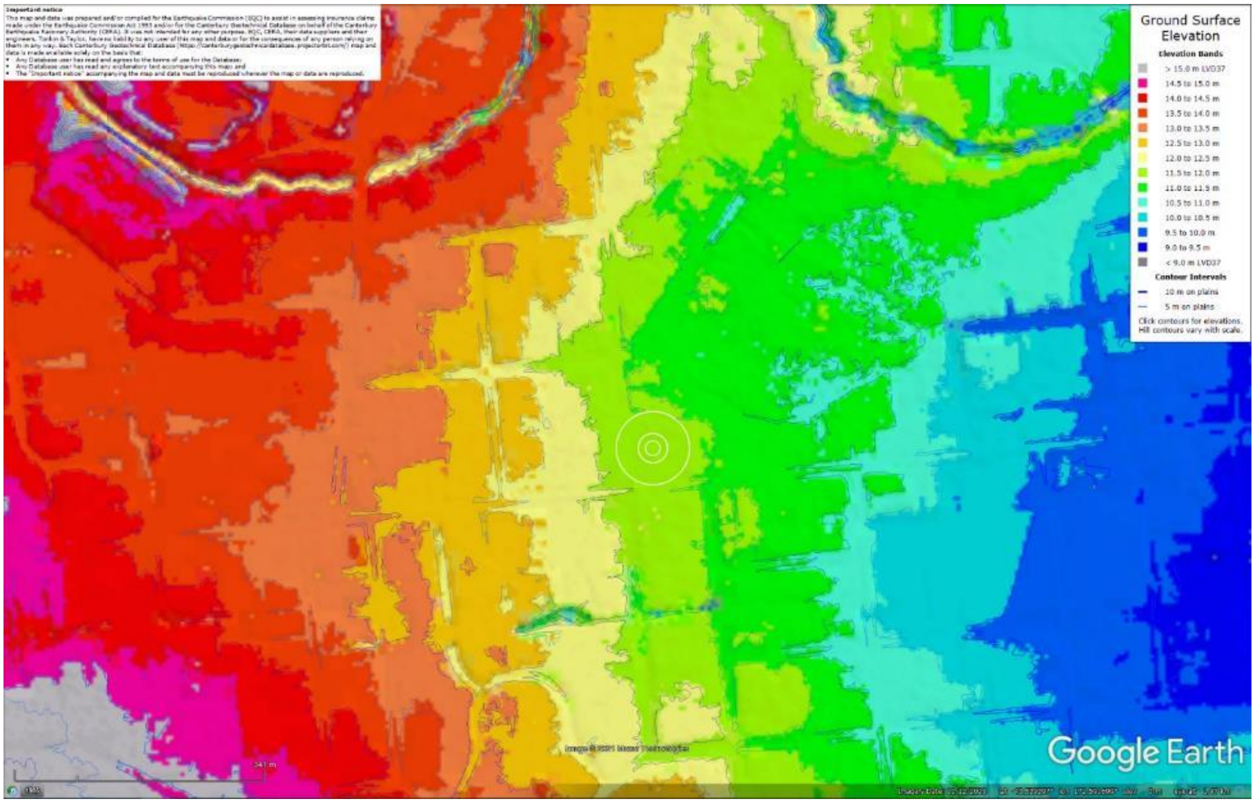

Figure 45: Ground surface elevation according to the Sep-11 LiDAR survey.

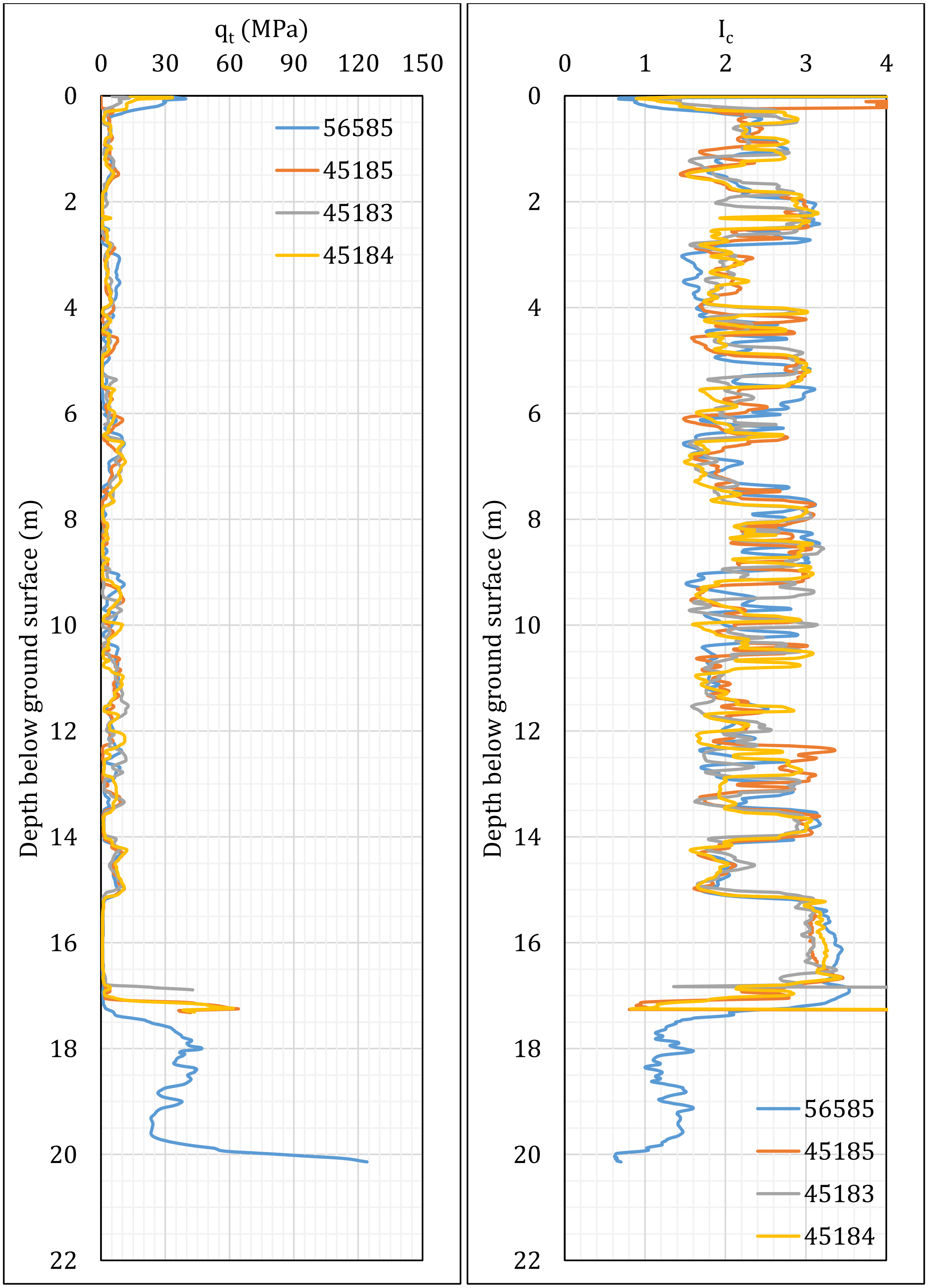

Figure 46: q_t and I_c profiles.

Note 6: The selection of CPTs for the area considered for settlement assessment (Figure 1) is based on the proximity of the CPTs to the considered areas. In accordance with that, the following table shows CPTs that were used for the volumetric settlement analysis in *Cliq v.3.0.3.2*, a CPT soil liquefaction software developed by GeoLogismiki. (The average volumetric settlements were reported in Table 8.)

Table 12: CPT profiles used in volumetric settlement analysis for areas selected for settlement assessment.

CPT ID No.	Patch A	Patch B	Road
57345	✓	✓	✓
45185	✓	✓	✓
45183			✓
45184			✓

Table 13: CPT-based results.

		CPT ID			
EQ Event	Parameter	57345	45185	45183	45184
Sep-10	S_{V1D} (mm)	213	204	201	215
	LSN	31	34	34	36
	LPI	14	15	14	15
	LPI_{ish}	8	7	7	10
	$D_{FS<1}$ (m)	1.68	2.71	1.88	2.50
Feb-11	S_{V1D} (mm)	234	225	228	238
	LSN	38	42	42	43
	LPI	24	24	25	26
	LPI_{ish}	16	17	18	19
	$D_{FS<1}$ (m)	1.52	1.00	1.16	1.22
Jun-11	S_{V1D} (mm)	81	79	68	72
	LSN	11	12	11	12
	LPI	1	1	1	1
	LPI_{ish}	0	1	0	0
	$D_{FS<1}$ (m)	4.62	11.89	5.56	8.06
Dec-11	S_{V1D} (mm)	61	60	49	53
	LSN	8	9	8	9
	LPI	1	1	0	1
	LPI_{ish}	0	0	0	0
	$D_{FS<1}$ (m)	undet.	undet.	8.90	8.08

Notes: $D_{FS<1}$ = Depth to the first liquefiable layer (FS_L<1) that is at least 200-mm thick, as determined by the Boulanger and Idriss (2016) liquefaction-triggering procedure (P_L=50%, C_{FC}=0.13, and $I_{c,cutoff}$ =2.6), and exported from *Cliq v.3.0.3.2*; undet. = the specified soil layer was not detected.

Note 7: Based on the borehole log BH 57241 (Figure 1), the groundwater table is at a depth of 4.6 m below the ground surface. The soil profile consists of (1) sandy fine to coarse gravel, GW, the fill below asphalt, to a depth of 0.25 m, (2) silt, ML, to a depth of 10.4 m, (3) silty sand, SM, to a depth of 10.95 m, (4) fine to medium sand, SP, to a depth of 11.75 m, (5) silt, ML, to a depth of 14.35 m, (6) fine sand, SP, to a depth of 15.1 m, (7) silt, ML, to a depth of 15.65 m (the end of the borehole). All soil layers (except the fill) are the Yaldhurst members of the Springston formation. Trace organics are present nearly throughout the entire soil profile. The borehole log BH 45186 (Figure 1) lists the following soil profile layers: (1) silt to a 2.5-m depth, (2) sand to a 10.2-m depth, (3) gravel to a 14.7-m depth, (4) sand to a 16.5-m depth, (5) silt to a 17.4-m depth, and (6) gravel to a 30.5-m depth.